Contents lists available at ScienceDirect

Agricultural and Forest Meteorology

Understory CO$_2$, sensible heat, and latent heat fluxes in a black spruce forest in interior Alaska

Hiroki Ikawa [a,f,*], Taro Nakai [a,b], Robert C. Busey [a], Yongwon Kim [a], Hideki Kobayashi [c], Shin Nagai [c], Masahito Ueyama [d], Kazuyuki Saito [e], Hirohiko Nagano [a], Rikie Suzuki [c], Larry Hinzman [a]

[a] International Arctic Research Center, University of Alaska Fairbanks, Fairbanks, AK 99775-7340, USA
[b] Hydrospheric Atmospheric Research Center, Nagoya University, Nagoya, Aichi 464-8601, Japan
[c] Department of Environmental Geochemical Cycle Research, Japan Agency for Marine-Earth Science and Technology, Yokohama, Kanagawa 236-0001, Japan
[d] Graduate School of Life and Environmental Sciences, Osaka Prefecture University, Sakai, Osaka 599-8531, Japan
[e] Department of Integrated Climate Change Projection Research, Japan Agency for Marine-Earth Science and Technology, Yokohama, Kanagawa 236-0001, Japan
[f] Agro-Meteorology Division, National Institute for Agro-Environmental Sciences, Tsukuba, Ibaraki 305-8604, Japan

ARTICLE INFO

ABSTRACT

An open black spruce forest, the most common ecosystem in interior Alaska, is characterized by patchy canopy gaps where the forest understory is exposed. This study measured CO$_2$, sensible heat, and latent heat fluxes with eddy covariance (EC) in one of those large canopy gaps, and estimated understory fluxes in a black spruce forest in 2011–2014. Then understory fluxes and ecosystem fluxes were compared. The understory fluxes during the snow-free seasons were determined by two approaches. The first approach determined understory fluxes as the fluxes from the canopy gap, assuming that fluxes under the canopy crown also had the same magnitude as the canopy gap fluxes. The second approach determined the understory fluxes by scaling canopy gap fluxes with a canopy gap fraction, assuming that only canopy gaps, which mostly constitutes the forest floor, contribute to fluxes. The true understory fluxes would be in between these two estimates. Overall, the understory accounted for 53% (39–66%), 61% (45–77%), 63% (45–80%), 73% (56–90%), and 79% (59–98%) of the total net ecosystem productivity (NEP), gross primary productivity (GPP), ecosystem respiration (RE), sensible heat flux (H), and latent heat flux (LE), respectively. The ratio of understory NEP (NEP$_U$) to the ecosystem NEP (NEP$_E$) and similarly calculated LE$_U$/LE$_E$ during the daytime increased with vapor pressure deficit (VPD) at low VPD conditions ($\sim$2000 Pa) at half-hourly temporal scale. At high VPD conditions, however, NEP$_U$/NEP$_E$ decreased with VPD, whereas LE$_U$/LE$_E$ was maintained at the high level even at high VPD conditions. Despite large ranges of the estimates for the understory contributions, we conclude that the understory plays an important role in the carbon and energy balances of the black spruce ecosystem, and their contribution highly depends on the level of VPD.

1. Introduction

Boreal forests account for about 25% of the global forest area (Food and Agriculture Organization, 2005) and are responsible for 8% of the carbon exchange throughout global terrestrial ecosystems (McGuire et al., 1997). As a result, their role in the global climate system is of particular interest. Long-term (several months to a decade) monitoring in boreal forests in the past few decades helped us understand the magnitude of CO$_2$ and energy fluxes and their temporal patterns, as well as their environmental responses (Black et al., 1996; Goulden et al., 1997; Iwata et al., 2012; Jarvis et al., 1997; Ueyama et al., 2014, 2009). In spite of decades of investigation on boreal forest carbon and energy balances, quite little is known about the role of the forest floor.

The understory of northern coniferous boreal forests can be a major determinant of carbon and energy balances in high-latitude regions. Generally, their forest floor receives a significant fraction

* Corresponding author at: Agro-Meteorology Division, National Institute for Agro-Environmental Sciences, Tsukuba, Ibaraki 305-8604, Japan.
E-mail address: hikawa.biomet@gmail.com (H. Ikawa).

of radiation due to their low tree stand density (Baldocchi et al., 2000a). This suggests high portions of carbon and energy fluxes contributed by the understory. In such ecosystems, it is necessary to consider the overstory and understory separately for accurately evaluating environmental influences on mass and energy exchanges between the atmosphere and ecosystems (Baldocchi et al., 2000b). Past studies reported that the understory in boreal forests contributes substantially to CO_2 and energy exchanges over boreal forests (Baldocchi et al., 1997a, 1997b; Baldocchi and Vogel, 1996; Bergeron et al., 2009; Black et al., 1996; Goulden and Crill, 1997; Heijmans et al., 2004; Iida et al., 2009; Xue et al., 2011). The forest floor is often a net source of CO_2 even if the ecosystem as a whole is a net sink, however.

Important factors that determine the understory fluxes include not only the available energy at the forest floor but also geographic characteristics, climate and plant community, and their influences most likely differ in time and space (Baldocchi et al., 2000a, 2000b; Heijmans et al., 2004; Misson et al., 2007; Xue et al., 2011). For example, Misson et al. (2007), based on the archived data from multiple sites in FLUXNET, reported that the interspatial variations in gross primary productivity in forest understories were positively related to light availability and leaf area index (LAI) of the understory species. Note that Misson et al. (2007)'s interspatial comparison was not limited to boreal forest though. On the other hand, Bergeron et al. (2009) reported that the understory contribution to photosynthesis decreased in the mid-summer, concluding that the fraction of understory photosynthesis was primarily determined by the extent of desiccation inferred by vapor pressure deficit (VPD) rather than light availability for the bryophyte-dominated understory in a black spruce forest.

Environmental responses are expected to be different between the overstory and understory. The overstory and understory have different structures and plant functional types; therefore, they are expected to have different characteristics in gas exchanges and energy partitioning (Baldocchi et al., 2000b; Iida et al., 2009). In response to ongoing environmental changes, different environmental responses between the overstory and understory would have nonlinear impacts on ecosystem growth, succession patterns, and regional energy balance (Hart and Chen, 2006; Tsuyuzaki et al., 2008). Therefore, it is necessary to evaluate the differences in the environmental responses between the overstory and understory to improve the current and future estimations of the regional and global carbon and energy balances.

An open black spruce forest is extremely common in the poorly drained, cold terrain of the subarctic region in North America (Viereck et al., 1992), and the understory components comprise a large proportion of the landscape (Fig. 1). Bergeron et al. (2009) and Goulden and Crill (1997) measured CO_2 exchange of understory components in different black spruce forests in Canada, and both studies reported that the understory contributed to 10–50% of photosynthesis and nearly 90% of respiration in the ecosystem. While these studies posed an importance of the understory, their understory measurements were limited to bryophytes with the chamber methods. In a typical black spruce forest in Alaska, shrubs also represent a significant portion (~20%) (Ruess et al., 2003). Furthermore, the relatively dense forests (overstory LAI = 3–5 m^2/m^2) reported in their studies most likely demonstrate different understory characteristics than open black spruce forests typical to interior Alaska.

With a goal to improve understanding of the role of the understory in the carbon and energy budgets of open black spruce forests in interior Alaska, the objectives of this study were to estimate the contributions from the forest understory to CO_2 and energy fluxes in the black spruce forest, and to compare the environmental responses between the whole ecosystem and its understory. To estimate the understory fluxes, we utilized the fact that an open
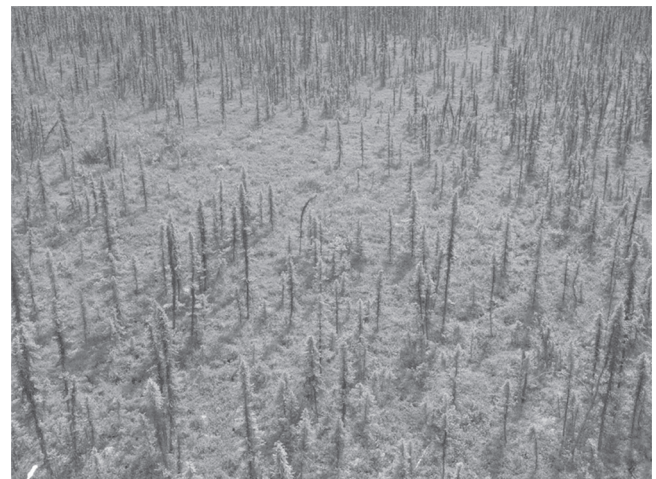

Fig. 1. The study site facing south from the eddy covariance tower (photo taken by TN on 7/6/2011). Extensive areas of interior Alaska are covered with sparse spruce forests.

black spruce forest typically consists of large canopy gaps within which the operation of eddy covariance (EC) is applicable. Then, we hypothesized the extent of the understory contributions to net ecosystem productivity (NEP) and latent heat flux (LE) depend on the level of VPD. This is because *Sphagnum* moss, which dominates the understory of the study site, is particularly sensitive to desiccation (Bergeron et al., 2009; Murray et al., 1989), and their response to VPD is most likely different from that of the canopy species.

2. Materials and methods

2.1. Study site

The JICS (JAMSTEC-IARC Collaboration Study) supersite (65°07′24″N, 147°29′15″W) was established in 2009 at an open black spruce (*Picea mariana*) forest. This site was established within the property of the Poker Flat Research Range (PFRR) of the University of Alaska Fairbanks to understand carbon and hydrological cycles in the boreal forest and promote interdisciplinary Subarctic research (Nakai et al., 2013; Sugiura et al., 2011; Suzuki et al., 2015). A 17-m scaffold tower hosts an EC system for CO_2 and energy fluxes and other meteorological measurements.

LAI of the overstory, considering clumping index, is 0.73 (Kobayashi et al., 2014). A cumulative basal area inflection (CuBI) height, also an aerodynamically effective canopy height, is 2.91 m (Nakai et al., 2013, 2010). The stem density of trees higher than 1.3 m was 3967 trees ha^{-1} (Nakai et al., 2013). The last major disturbance (i.e., forest fire) at the site was about 100 years ago, and an average stand age was 67 years as of 2012 (Ueyama et al., 2015). Considering the stand age, canopy height, and density, the ecosystem is best classified as an open black spruce forest (1.A.2.f) in Viereck et al. (1992)'s vegetation classification for Alaska.

The understory within a typical footprint of EC is predominated by peat moss (*Sphagnum fuscum*) and feather moss (*Hylocomium splendens*). These cover 27% of the floor surface, though they also reside under shrubs and sedges. Shrubs, which mainly include Labrador tea (*Ledum groenlandicum*), bog bilberry (*Vaccinium uliginosum*), cloudberry (*Rubus chamaemorus*), and bog birch (*Betula glandulosa or Betula nana*) account for 27% of the floor surface. Sedges, mostly identified as cotton grass (*Eriophorum vaginatum*), form tussocks, covering 24% of the floor surface. Northern reindeer lichen (*Cladina stellaris*) often forms a colony, covering 13% of the ground surface. Bare peat ground and dead plants cover 9% of the surface.

Table 1
The periods of snow-covered, snow-disappearing, snow-free, and snow-covering seasons for an open black spruce forest at the Poker Flat Research Range in interior Alaska.

Year	Snow-covered	Snow-disappearing	Snow-free	Snow-covering
2011	Until 4/24, from 10/18	From 4/25 to 5/18	From 5/19 to 9/11	From 9/12 to 10/17
2012	Until 4/13, from 10/16	From 4/14 to 5/28	From 5/29 to 9/7	From 9/8 to 10/15
2013	Until 5/8, from 11/2	From 5/9 to 6/18	From 6/19 to 9/17	From 9/18 to 11/1
2014	Until 4/19, from 10/5	From 4/20 to 5/11	From 5/12 to 9/24	From 9/25 to 10/4

2.2. Snow-free seasons

We determined snow-free seasons based on images obtained by a digital camera system (Coolpix 4500; Nikon, JAPAN) with a fisheye lens (FC-E8; Hayasaka Rikoh, JAPAN) mounted on the top of the scaffold tower (Nagai et al., 2013) (Table 1). This study focused on snow-free season; however, other seasons (snow-disappearing, snow-covering, and snow-covered seasons) were also determined for the purpose of quality controls of EC data.

Snow-disappearing seasons were determined from the day when 10% of the ground snow had melted until the day the ground was totally snow-free. Snow-covering seasons were determined from the first snow day until the day when the ground was continuously covered until the beginning of the next snow-disappearing season.

2.3. Eddy covariance for the ecosystem and canopy gap

NEP, sensible heat flux (H), and latent heat flux (LE) were measured with the EC technique both for the ecosystem and a canopy gap. NEP is a net CO_2 flux where the sink of CO_2 indicates a positive value. The EC for the ecosystem was operated on a scaffold tower at a vertical height of 11 m. The EC system on a 1.9 m tripod was securely located 15 m apart from the scaffold tower in a relatively wide canopy gap where the understory compositions were exposed. Storage terms for NEP, H, and LE were estimated based on the data at the measurement height and added for the flux calculation for EC at both 11 m and 1.9 m. The storage term is generally negligible for an EC with a short measurement height (i.e., inside forest) (e.g., Misson et al., 2007), though the term was also applied to EC at 1.9 m to avoid any potential bias between the two sets of EC data. The calculations of latent heat for evapotranspiration (when air temperature >0 °C) and sublimation (when air temperature <0 °C) were done following Fritschen and Gay (1979).

Mixing ratios of CO_2 and H_2O, three-dimensional wind speed, and sonic temperature were continuously sampled at 10 Hz and stored in a laptop at the site. CO_2 and H_2O signals were measured with an enclosed infrared gas analyzer (LI-7200, LI-COR, USA). The LI-7200 gas analyzer has advantages over open-path type gas analyzers for computing accurate CO_2 and H_2O mixing ratios by detecting pressure of the sample air stream at high frequency, as well as avoiding the self-heating effect (Burba et al., 2012, 2008; Nakai et al., 2011). Wind speed and sonic temperature were measured with a sonic anemometer (WindMaster Pro, Gill, UK).

High-frequency data were processed to calculate fluxes with EddyPro (ver. 5.2.2, LI-COR, USA) (Fratini and Mauder, 2014). Data spikes in 10-Hz data were removed following Vickers and Mahrt (1997). Errors in the WindMaster Pro anemometer depending on angle-of-attack were corrected for wind velocity (Nakai et al., 2014, 2006; Nakai and Shimoyama, 2012). The correction for the loss of fluxes at high frequency was applied following Moncrieff et al. (1997).

After data were half-hourly averaged, they were filtered out based on apparently high or low CO_2 mixing ratio or sonic temperature associated with sensor malfunctions (0.3%, 0.7%: hereafter, percentages in brackets represent the amount of data filtered out

at each step for EC at 11 m and 1.9 m, respectively, in snow-free seasons); apparently high variance of CO_2 signal, vertical wind velocity or sonic temperature (5%, 13%); outliers in H + LE larger than the highest Rn – G (difference between net radiation and ground heat flux) for each snow-based season (see Section 2.2 for the definition of snow-based seasons) (0.1%, 0.1%); data with low friction velocity when energy closure achieved less than 50% (30%, 41%; Iwata et al., 2012); outstanding negative spikes in LE less than $-50 \, W \, m^{-2}$ that occurred with undetermined causes (0.06%, 0.02%); and outliers larger or smaller than the median of 85% data ± 5 standard deviations for daytime (6:00–21:00 AST) and night time for each season after all other quality controls (2%, 0.4%). The threshold of friction velocity was determined to be $0.15 \, m \, s^{-1}$ with the EC data at 11 m, and the same threshold was applied for the EC data at 1.9 m. For canopy gap fluxes, data were further filtered out when the wind direction was not oriented to the target canopy gap (180°–270°), which often occurred at night (21%). As a result, 63% and 23% of EC data were regarded as good quality for the ecosystem and the canopy gap, respectively.

Flux partitioning to calculate gross primary productivity (GPP) and respiration (RE) were performed, using empirically estimated RE from nighttime data with the function suggested by Lloyd and Taylor (1994) with Flux Analysis Tool (FAT) (http://www.japanflux.org/software_E.html) (Ueyama et al., 2012). The detail in flux partitioning is available in Ueyama et al. (2012). All data used in this study are quality-controlled and not gap-filled.

2.4. Estimation of understory fluxes

For estimating understory fluxes, we were not able to set an EC system under the forest canopy to directory measure understory fluxes like other EC studies on the forest understory (e.g., Baldocchi and Vogel, 1996) because black spruce trees do not have a clear separation between the canopy crown and trunks. Instead, we estimated understory fluxes based on the canopy gap fluxes.

The understory fluxes during the snow-free season were estimated by two approaches. The first approach determined understory fluxes (F_U) as the fluxes from the canopy gap measured at the vertical height of 1.9 m ($F_{1.9}$). This method assumes that the flux under the canopy crown had the same magnitude as that from the canopy gap (i.e., $F_U = F_{1.9}$).

The second approach determined understory fluxes by scaling canopy gap fluxes with a canopy gap fraction within the footprint of the EC at 11 m (α_{11}), assuming that only canopy gaps contribute to the understory flux (i.e., $F_U = \alpha_{11} F_{1.9}$). The true understory fluxes would be in between these two estimates; therefore, they provide the upper and lower limits of the estimates for understory fluxes.

The α_{11} was determined on a satellite image by a 2-D footprint model used in Matthes et al. (2014). This footprint model was based on Hsieh et al. (2000) and was spatially extended following Detto et al. (2006). A panchromatic QuickBird-2 satellite image obtained at 21:27 UTC (12:27 AST) on September 29th, 2009 was used to identify tree stands at the spatial resolution of 0.65 m (Fig. 2). The satellite image was provided by the Polar Geospatial Center at the University of Minnesota after atmospheric and orthogonal corrections were applied. The digital number (DN) of 800 reasonably
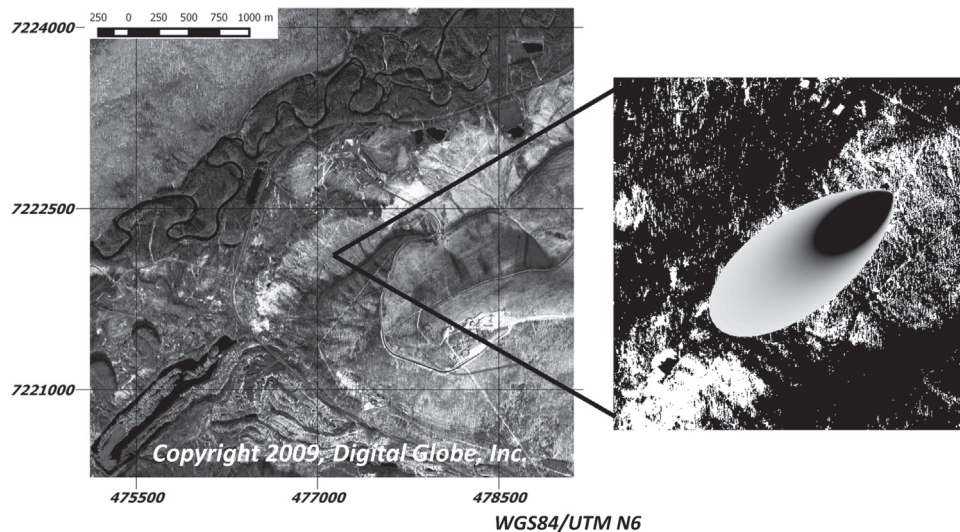
Fig. 2. Canopy gap fraction analysis was performed using a satellite image (Quickbird-2 panchromatic image obtained at 21:27 UTC on September 27, 2009). The footprint area in the figure is for the EC at 11 m at 12:00 AST, June 5, 2013. The gray scale in the footprint indicates a relative strength of the signal source. The Quickbird-2 image was obtained from the Polar Geospatial Center of the University of Minnesota.

separated tree stands (DN < 800) and forest floor (DN > 800). During the snow free seasons, average α_{11} was 0.55 ($\pm$0.11 SD, $N = 6763$). Similarly estimated, the average gap fraction for the footprint of the canopy gap flux ($\alpha_{1.9}$) was 0.89 ($\pm$0.04 SD, $N = 4129$), indicating that the EC signals for the canopy gap were slightly contaminated by the components of black spruce trees.

The α_{11} can change by solar angle when the remote sensing image was captured. However, $\alpha_{11} = 0.55$ well agreed with an average canopy gap fraction during the snow-free season estimated by a plant canopy analyzer (LI-2000, LI-COR, USA) (unpublished data).

The contributions of understory to each flux were quantified by the slopes of the regression lines with a zero interception for the understory and ecosystem fluxes, approximating that understory fluxes become zero when the total fluxes are zero. Standard deviation of the understory contributions were calculated by bootstrapping the sampling data pool and reconstructing the regression 100 times.

2.5. Other meteorological measurements

Air temperature and relative humidity were measured at 1.5 m above the ground with a humidity and temperature probe (HMP-155C, Vaisala, Finland) installed in a ventilated double-walled tube. Atmospheric pressure was measured near the ground with a barometer (PTB110, Vaisala, Finland). Wind direction was measured with a wind vane (020C, MetOne, USA) mounted at 17 m on the tower. Net radiation was measured at 16 m with a CNR4 pyranometer (Kipp & Zonnen, The Netherlands). Ground heat flux was measured with a heat flux plate (HFP01SC, Hukseflux, The Netherlands) at 8-cm depth in the moss layers at two locations. Photosynthetic photon flux density (PPFD) was measured with a quantum sensor at 16 m (LI-190, LI-COR, USA). Soil temperature and volumetric soil water content were measured at 5 and 10 cm below the ground surface with a thermistor (CS107, Campbell Sci., USA) and a water content reflectometer (CS616, Campbell Sci., USA), respectively. Volumetric soil water content was normalized by the maximum and minimum value for each year. In this study, soil temperature and moisture data at 10 cm were used only when the measurement at 5 cm failed. Rain/snow precipitation was measured with a rain gauge (RS-222A, Ogasawara Keiki, JAPAN), and snow depth was measured with a sonic ranging sensor (SR50A, Campbell Sci., USA) at three locations. Raw data output from the

snow depth sensor showed consistently positive values even during snow-free seasons, and the minimum values recorded during the snow-free seasons were regarded as the artificial offset and subtracted from data collected each year.

Air temperature, VPD, wind speed, and wind direction due to system malfunction were gap-filled with data obtained from the EC system (6%; hereafter percentages in brackets represent the amount of data gap-filled). Precipitation data were gap-filled with the data collected at the Fairbanks international airport (0.2%). Soil moisture and PPFD data were gap-filled with data obtained from an adjacent meteorological station (Iwata et al., 2011), courtesy of Dr. Yoshinobu Harazono (Osaka Prefecture University) after constructing linear regression models for each season (5%). Missing data for net radiation was estimated from PPFD for each season (5%). Soil temperature and ground heat flux were gap-filled by constructing multi-linear regression models using all other meteorological data (5%).

2.6. VPD responses of the understory contributions to NEP and LE

Understory fluxes estimated by two methods (see Section 2.4) essentially showed very similar temporal patterns and environmental responses, and hence the average of the two methods was used for the correlation analysis. Since air temperature was tightly correlated to VPD at a half-hourly scale ($R = 0.82$), it was not possible to delineate those effects on NEP or LE. High VPD (3000 Pa) was exclusively concurrent with high air temperature, and their correlation was particularly high ($R = 0.89$). Consequently, examined relationship between VPD and fluxes includes the air temperature effect as well.

3. Results and discussion

3.1. Meteorological conditions

Overall, 2011 and 2012 had similar meteorological conditions, and 2013 and 2014 were characterized as hot and wet summer, respectively (Fig. 3). Seasonal amplitudes of daily air temperature in 2011–2012 and 2014 were similar to the long-term average recorded in the adjacent city of Fairbanks (Shulski and Wendler, 2007). The year 2013 was characterized by late snowmelt and high VPD and air temperature. Half-hourly VPD reached up to 4993 Pa
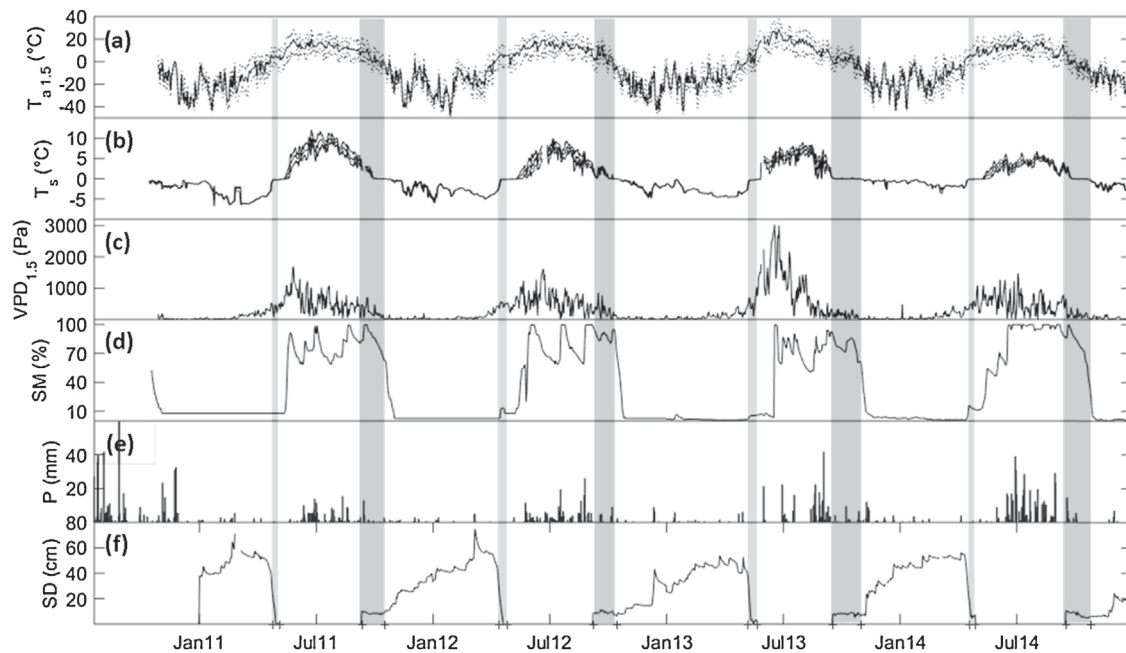
Fig. 3. Meteorological conditions observed in an open black spruce forest at the JICS supersite, Alaska, USA, October 2010- December 2014. (a) $T_{a1.5}$ is air temperature measured at 1.5 m above the ground, (b) T_S, soil temperature, (c) $VPD_{1.5}$, vapor pressure deficit measured at 1.5 m above the ground, (d) SM, normalized soil moisture, (e) P, precipitation, (f), and SD, snow depth. Shadows represent snow-disappearing periods and snow-covering periods.

on June 25, 2013. Further, our highest daily average temperature of 29 °C on June 26 was higher than normal high temperature (24 °C) in Fairbanks during 1906–2004 (Shulski and Wendler, 2007). Although air temperature was highest in 2013 (daily average of 16 °C during the snow-free season), average daily soil temperature in snow-free season of 4.8 °C was similar to that in 2011–2012. Average soil surface temperature during the snow-free season was lowest (3.0 °C) in 2014. Normalized soil moisture increased rapidly after the snowmelt, decreased over time, and rapidly recovered at each rain event repeatedly during the snow-free seasons. Along with the dry and high-temperature conditions, normalized soil moisture dropped to around 50% in summer of 2013, and the average value during the snow-free season was 59%. Normalized soil moisture during the snow-free periods was highest in 2014, with an average value of 78%. High soil moisture in 2014 was attributed to heavy precipitation as annual precipitation of 514 mm was higher than the previous record high precipitation in Fairbanks in 1990 (470 mm). Precipitation in other 3 years ranged from 247 mm in 2011 to 375 mm in 2013.

3.2. Understory and ecosystem fluxes

Understory accounted for about half of CO_2 flux (i.e., NEP_E, GPP_E, and RE_E). Half-hourly understory NEP, GPP, and RE (i.e., NEP_U, GPP_U and RE_U) showed similar seasonal patterns as those of the total fluxes (Fig. 4). Overall, the understory flux assuming $F_U = F_{1.9}$ estimated the understory contributions at 66% ($\pm$0.5% SD) ($R^2 = 0.69$) for NEP_E, 77% ($\pm$0.5% SD) ($R^2 = 0.50$) for GPP_E, and 80% ($\pm$0.8% SD) ($R^2 = 0.22$) for RE_E, during the snow-free seasons in 2011–2014 (Fig. 5). Similarly, the understory contributions for NEP_E, GPP_E, and RE_E were 39% ($\pm$0.4% SD) ($R^2 = 0.65$), 45% ($\pm$0.3% SD) ($R^2 = 0.46$), and 45% ($\pm$0.4% SD) ($R^2 = 0.19$) by the second approach.

Regardless of the two methods, these results confirm that the understory had significant contributions to CO_2 fluxes at the ecosystem scale. The high contribution suggests that mosses at the forest floor account for a large fraction of ecosystem productivity (Bisbee et al., 2001; Grant et al., 2001; Oechel and Cleve, 1986), and may contribute the high understory productivity at our site.

In addition to bryophyte species, the canopy gap also consists of shrubs and very young black spruce trees, and their contributions would not be negligible as well.

The understory contribution to ecosystem respiration was also in part related to the root respiration that would account for about half the total soil respiration in a black spruce forest ecosystem (Ruess et al., 2003; Schuur and Trumbore, 2006). Low correlation coefficients between the ecosystem and understory respiration (Fig. 5) imply unique environmental controls on the understory respiration. Further study is desirable to quantify fluxes from different understory components, for example, by chamber methods (e.g., Heijmans et al., 2004) and isotopic methods (e.g., Schuur and Trumbore, 2006).

The understory contributions to the ecosystem productivity (NEP and GPP) decreased in the abnormal weather conditions (Fig. 4). The year 2013 was characterized by a repetitive freeze and thaw that most likely prevented the growth of understory vegetation in spring, and high temperature and VPD that likely inhibited the productivity of bryophyte in mid-summer (Bergeron et al., 2009). On the other hand, relatively low level of sunlight and frequently inundated ground surface would have decreased the vegetation growth at the forest floor in 2014. These results suggest a possibility that the understory was more sensitive to extreme weather than overstory black spruce trees. Despite these findings in NEP and GPP, our data were limited to 4 years and the difference in the understory contribution to GPP in relatively normal years of 2011 and 2012 was even larger than the difference between those in extreme years (2013 and 2014) and 2012. Further continuous observation is necessary to clarify the understory contributions in extreme climate.

The understory also contributed highly to energy exchange at the ecosystem scale. H_U contributed 56% ($\pm$0.3% SD, $R^2 = 0.89$)–90% ($\pm$0.4% SD, $R^2 = 0.90$) for H_E and LE_U, 59% ($\pm$0.4% SD, $R^2 = 0.74$)–98% ($\pm$0.6% SD, $R^2 = 0.77$) for LE_E during the snow-free seasons (Figs. 6 and 7). The understory contribution to LE was consistently higher than that to H in all years. This suggests that sensible heat exchanged at the tree crown more effectively than latent heat. Furthermore, black spruce needles have relatively low stomatal
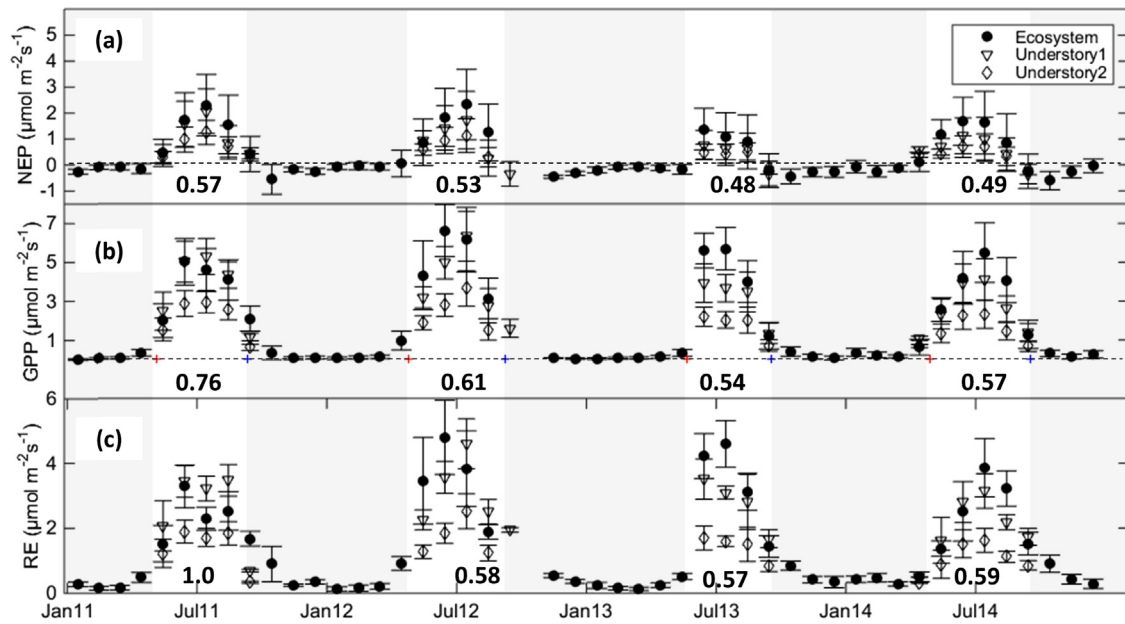
Fig. 4. Monthly average NEP (a), GPP (b), and RE (c) of the ecosystem and understory in 2011–2014 for an open black spruce forest at the Poker Flat Research Range in interior Alaska, USA. Understory fluxes were estimated by two approaches explained in Section 2.4. The numbers indicate an average contribution of understory to the ecosystem flux for each snow-free season. Note that the monthly average was calculated from the quality data without gap-filling by averaging 6-hour mean values for each month, and the error bar represents $(\sum v_h)^{1/2}/4$, where v_h is the variance for each 6-hour window.

conductance and partition more available energy to sensible heat flux than to latent heat flux (Grant et al., 2001; Jarvis et al., 1997). In addition, since the forest floor was water-logged or wet, the moss passively transferred vapor to the atmosphere at the surface without regulating transpiration by stomata. Despite high soil moisture, LE_U/LE_E was lowest in 2014 owing to low VPD, suggesting that the range of soil moisture within the measured range was not an apparent controlling factor for LE_U.

Understory contributions to the ecosystem CO_2 and energy fluxes were higher in this study than most other studies from evergreen forests (Table 2). The high understory contributions in this study would be attributed to a small LAI of the black spruce trees. It has to be emphasized that this sparse spruce forest composes a typical landscape in the interior Alaska. The high contributions of the understory reported in this study confirm the Baldocchi et al. (2000b)'s remark that sparse forests are dual source systems. The understory compositions in boreal forests are often associated with certain canopy species (Viereck et al., 1992), because the understory compositions are the strong determinants for decomposition and

nutrient flows (Nilsson and Wardle, 2005). However, the extent to which each component exists differs by locations. For example, a similar open black spruce forests in Fairbanks (Ueyama et al., 2014, 2006) has apparently more structurally developed shrubs and sedges. If the proportions of the understory components are to be changed by, for example, the shrub expansion occurring globally (Naito and Cairns, 2011), this will most likely change the contributions of the understory in black spruce forests.

3.3. Response to VPD

Both NEP_E and NEP_U during the daytime (10–15 Alaskan Standard Time) decreased as VPD increased, whereas both LE_E and LE_U increased asymptotically with VPD (Fig. 8). The bryophytes that dominate the understory do not have a stomatal regulation; however, it is commonly known that they decrease productivity under a dry condition (Bergeron et al., 2009; Murray et al., 1989). Additionally, high VPD also limits the productivity through stomatal
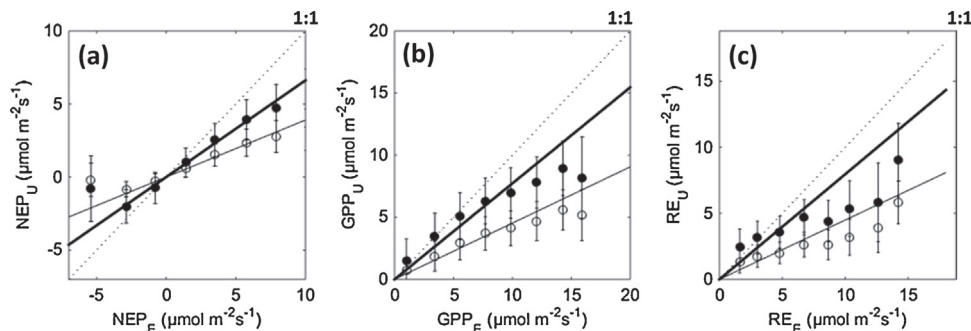

Fig. 5. The understory contributions were expressed by the ratios between the understory NEP, GPP, and RE (NEP_U, GPP_U, and RE_U) and ecosystem NEP, GPP, and RE (NEP_E, GPP_E, and RE_E) with the first method (bold lines and black circles) and the second method (thin line and white circles). The range of the understory contributions determined by the two methods were 39% ($\pm 0.4\%$ SD)–66% ($\pm 0.5\%$ SD) ($R^2 = 0.65$ and 0.69, respectively), 45% ($\pm 0.3\%$ SD)–77% ($\pm 0.5\%$ SD) ($R^2 = 0.46$ and 0.50, respectively), and 45% ($\pm 0.4\%$ SD)–80% ($\pm 0.8\%$ SD) ($R^2 = 0.19$ and 0.22, respectively) for NEP, GPP, and RE, respectively during the snow-free seasons in 2011–2014. Quality data without gap-filling in 2011–2014 were pooled and block averaged for each plot. Error bars in the figures represent standard deviation. Regressions were calculated for half-hourly data before the averaging.

Table 2

Understory contributions to CO_2 and energy fluxes in various boreal forests.

Understory contribution (%)					Ecosystem type	Canopy LAI	Understory spp.	Season	Method	Measurement height	Reference
NEP	GPP	RE	H	LE						Ecosystem/understory	
Deciduous forest											
–	32	–	–	22	Aspen	1.8	Hazel nuts	Annual	EC	39.5/4	(1)
–	–	–	–	25	Aspen	up to 5.6	Hazel nuts	Summer	EC	39/4	(2)
–	50	–	–	50	Larch	1.6–2.0	Cowberry	Summer	EC, model	32/3.3	(3)
–	–	–	–	51	Larch	1.6–2.0	Cowberry	Summer	EC	32/3.3	(4)
–	–	–	–	33–92	Larch	1.5	Small twigs, lichen	Summer	EC/lysimeter	21	(5)
–	50[*]	40	–	–	Larch	1.4	Cowberry	Summer	EC	21/1.8	(6)
Evergreen forest											
–	–	68[**]	–	20–40	Jack pine	1.9–2.2	Alder, bearberry, bog cranberry, lichen	Growing season	EC	20/1.8	(7,8)
–	–	20–30[***]	20–30	20–30	Jack pine	2.78–3.34	Alder, bearberry, bog cranberry, lichen	Summer	EC	44/2	(9)
–	10[****]	20[****]	–	10	Pine/spruce	3–4	Fens	Growing season	EC	102/2.5	(10)
25	–	–	–	–	Black spruce (closed canopy)		Feather moss, sphagnum moss	Annual	EC/model	29/ground	(11)
–	10–50	50–90	–	–	Black spruce (closed canopy)	4–5	Feather moss, sphagnum moss	Summer	EC/chamber	29/ground	(12)
–	17.5	86	–	–	Black spruce (closed canopy)	3.7	Shrub (sheep laurel, Labrador tea, alder), feather moss, sphagnum moss, lichen	Annual	EC, chamber	24/ground	(13)
53 (39–66)	61 (45–77)	63 (45–80)	73 (56–90)	79 (59–98)	Black spruce (open canopy)	0.73	Sphagnum moss, feather moss, lichen, shrub, sedge	Snow-free	EC	11/1.9	This study
Mixed forest											
–	33	–	–	–	Pedunculate oak, Scott pine	–	Rhododendron, cherry	Annual	Model	NA	(14)

(1) Black et al. (1996), (2) Blanken et al. (1997), (3) Xue et al. (2011), (4) Iida et al. (2009), (5) Kelliher et al. (1997), (6) Hollinger et al. (1998), (7, 8) Baldocchi et al. (1997a, 1997b), (9) Baldocchi and Vogel (1996), (10) Constantin et al. (1999), (11) Grant et al. (2001), (12) Goulden and Crill (1997), (13) Bergeron et al. (2009), (14) Sampson et al. (2006).

[*] Estimated by Xue et al. (2011).

[**] The magnitude of the variation compared to NEP.

[***] The magnitude of the variation compared to NEP.
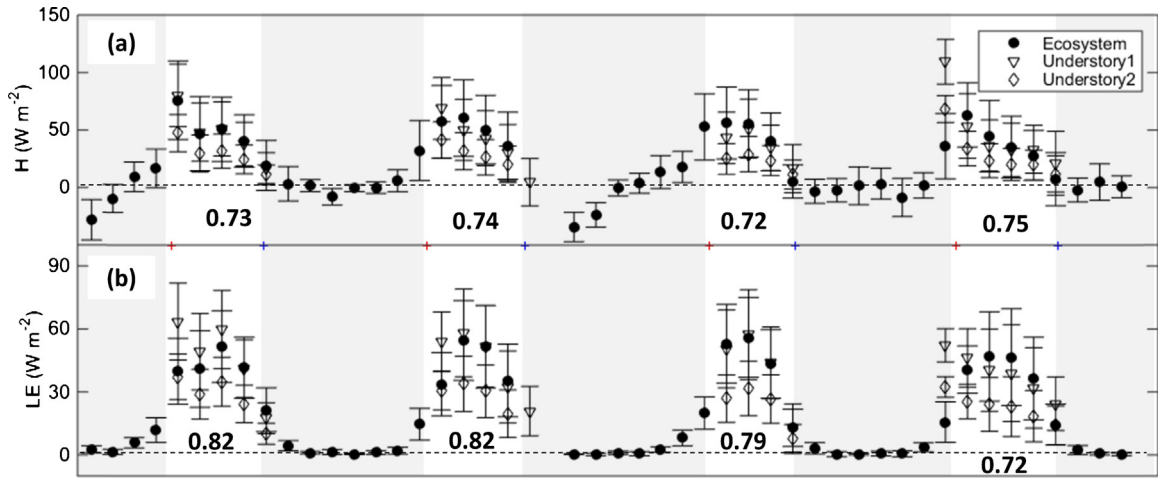
[****] Estimated from Fig. 7.

Fig. 6. Monthly average H (a) and LE (c) of the ecosystem and understory in 2011–2014 for an open black spruce forest at the Poker Flat Research Range in interior Alaska, USA. Monthly average values were also shown for snow-free seasons. Understory fluxes were estimated by two approaches explained in Section 2.4. The numbers indicate an average contribution of understory to the ecosystem flux for each snow-free season. Note that the monthly average was calculated from the quality data without gap-filling by averaging 6-hour mean values for each month, and the error bar represents $(\sum v_h)^{1/2}/4$, where v_h is the variance for each 6-hour window.

closure for other vascular plants (shrubs and sedges) inhabited in the understory.

Despite the strong correlation between air temperature and VPD, soil temperature and VPD were not correlated ($R = 0.07$), and subsequently, no clear relation was found between soil temperature and NEP$_U$. This implies that the negative effect of extreme VPD or air temperature on NEP likely reflects a decrease in the productivity of the understory vegetation rather than a change in soil respiration that highly depends on soil temperature at a site scale (e.g., Ruess et al., 2003; Vogel et al., 2005). The understory contribution to respiration was even lowest in warm 2013 (Fig. 4). Nevertheless, we suggest a further detail research on the magnitudes and environmental controls on root respiration at our study site because the control of soil temperature on root respiration may not be generalized without considering other controlling factors, such as organic matter, moisture, and nitrogen availability (Schuur and Trumbore, 2006; Vogel et al., 2005).

The response of understory contributions in NEP (NEP$_U$/NEP$_E$) to VPD varied with different VPD levels (Fig. 9a). At relatively low VPD up to 2000 Pa, NEP$_U$/NEP$_E$ increased with VPD, but the relation was reversed at high VPD. Fig. 8 also indicates that low NEP$_U$/NEP$_E$ at high VPD was not related to soil temperature. The optimum curve for NEP$_U$/NEP$_E$ and VPD suggests a possibility that the understory productivity is vulnerable to dry or dampened conditions. This is consistent with overall low NEP$_U$ and GPP$_U$ in dry 2013 and wet 2014 (Fig. 4). Euskirchen et al. (2014) also reported a decrease in NEP in a similar black spruce forest at high air temperature, which was likely concurrent with high VPD in 2013. With the results obtained here, we speculate that the decrease in NEP in their study was most likely attributed to the decrease in understory productivity.

While the understory contribution to NEP (i.e., NEP$_U$/NEP$_E$) showed a parabolic curve and dropped at high VPD, the understory contribution to LE (LE$_U$/LE$_E$) asymptotically increased with
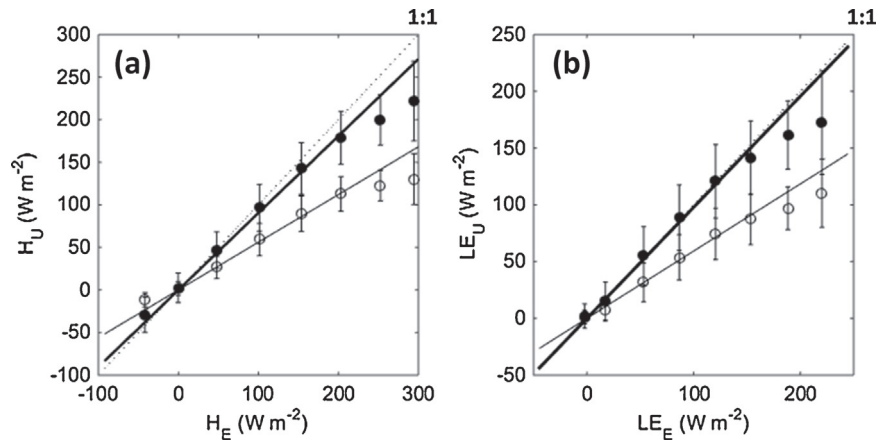

Fig. 7. The understory contributions were expressed by the ratios between the understory H and LE (H_U and LE$_U$) and ecosystem H and LE (H_E and LE$_E$) with the first method (bold lines and black circles) and the second method (thin line and white circles). The range of the understory contributions determined by the two methods were 56% ($\pm0.3\%$ SD)–90% ($\pm0.4\%$ SD) ($R^2 = 0.89$ and 0.90, respectively) and 59% ($\pm0.4\%$ SD)–98% ($\pm0.6\%$ SD) ($R^2 = 0.74$ and 0.77, respectively) for H and LE, respectively during the snow-free seasons in 2011–2014. The data in 2011–2014 were pooled and block averaged for each plot. Error bars in the figures represent standard deviation. Regressions were calculated for the half-hourly data before the averaging.
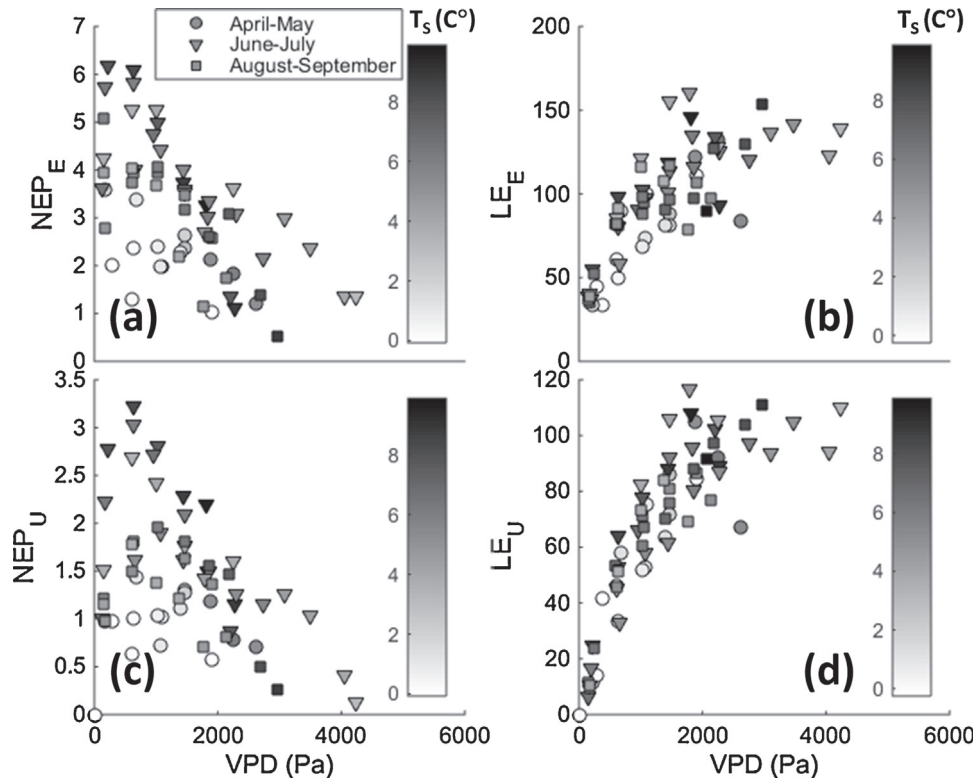
Fig. 8. Both NEP for the ecosystem (NEP_E) and understory NEP (NEP_U) decreased with VPD (a, c) and both LE for the ecosystem (LE_E) and understory LE (LE_U) increased with VPD (b, d). High VPD was concurrent with high air temperature but not necessarily with soil temperature (T_S). Each point represents a binned average of half-hourly quality data without gap-filling during the daytime (10–15 AST) for early (April–May with ●), mid (June–July, ▼), and late (August–September, ■) growing stages for each year in 2011–2014. Note that average understory fluxes estimated by the two methods explained in Section 2.4 are used here.
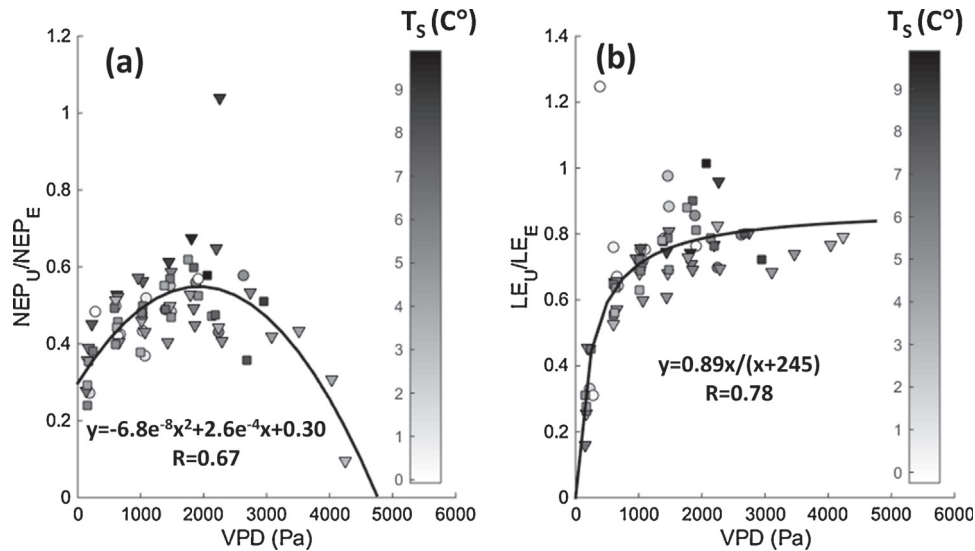
Fig. 9. The ratio of understory NEP (NEP_U) and NEP for the ecosystem (NEP_E), increased with VPD at low VPD (up to 2000 Pa) and decreased at higher VPD (a). The ratio of LE (LE_U/LE_E) increased asymptotically with VPD (b). High VPD was concurrent with high air temperature but not necessarily with soil temperature (T_S). Each point represents a binned average of half-hourly quality data without gap-filling during the daytime (10–15 AST) for early (April–May, marked with ●), mid (June–July, ▼), and late (August–September, ■) growing stages for each year in 2011–2014. Note that average understory fluxes estimated by the two methods explained in Section 2.4 are used here.

VPD and maintained at the high level at high VPD (Fig. 9b). Relatively high LE_U at high VPD was attributed to the moist and partly water-logged ground surface. Therefore, the understory contribution to LE in 2013 was comparable with other years, despite the low level of soil moisture.

4. Conclusion

This study quantified the understory contribution to CO_2 and energy fluxes in the open black spruce forest in interior Alaska and investigated how the understory contributions differed at

different VPD levels. Two approaches were provided to estimate the understory fluxes depending on whether $F_U = F_{1.9}$ or $F_U = \alpha_{11} F_{1.9}$, providing upper and lower limitations of the estimates. Despite large differences in the two estimates, it was confirmed that the understory represented large fractions of CO_2 and energy fluxes. Therefore, to accurately estimate current and future CO_2 and energy balances in the black spruce forest, one must consider overstory and understory components differently. To further refine the estimates of the understory contributions, it is desirable to quantify how the understory fluxes differ by each understory component, including bryophytes, shrubs, sedges, very young spruce trees, tree roots, and microbial communities.

We also conclude that the understory responses to VPD were different with those of the overstory. In our study, the understory contribution to NEP (NEP_U/NEP_E) showed an optimum curve with respect to VPD, and LE_U/LE_E asymptotically increased with VPD. High LE_U was attributed to the moist and partly water-logged ground surface. Low NEP_U/NEP_E in low and high VPD at half-hourly scale likely reflected relatively low NEP_U and GPP_U in dry 2013 and wet 2014. Thus, it is possible that the understory was more vulnerable to extreme weathers than black spruce trees. Nevertheless, since our data set is limited to 4 years only, further continuous monitoring on both ecosystem and understory fluxes together with better clarification of carbon inventory is necessary to clarify how the inter-annual climate variability affects the contributions of the understory in an open black spruce forest ecosystem.

Acknowledgements

References

Baldocchi, D.D., Vogel, C.A., 1996. Energy and CO_2 flux densities above and below a temperate broad-leaved forest and a boreal pine forest. Tree Physiol. 16, 5–16.

Baldocchi, D.D., Vogel, C.A., Hall, B., 1997a. Seasonal variation of energy and water vapor exchange rates above and below a boreal jack pine forest canopy. J. Geophys. Res. Atmos. 102, 28939–28951, http://dx.doi.org/10.1029/96JD03325

Baldocchi, D.D., Vogel, C.A., Hall, B., 1997b. Seasonal variation of carbon dioxide exchange rates above and below a boreal jack pine forest. Agric. For. Meteorol. 83, 147–170, http://dx.doi.org/10.1016/S0168-1923(96)02335-0

Baldocchi, D., Kelliher, F.M., Black, T.A., Jarvis, P., 2000a. Climate and vegetation controls on boreal zone energy exchange. Glob. Change Biol. 6, 69–83, http://dx.doi.org/10.1046/j.1365-2486.2000.06014.x

Baldocchi, D., Law, B.E., Anthoni, P.M., 2000b. On measuring and modeling energy fluxes above the floor of a homogeneous and heterogeneous conifer forest. Agric. For. Meteorol. 102, 187–206, http://dx.doi.org/10.1016/S0168-1923(00)00098-8

Bergeron, O., Margolis, H.A., Coursolle, C., 2009. Forest floor carbon exchange of a boreal black spruce forest in eastern North America. Biogeosciences 6, 1849–1864.

Bisbee, K., Gower, S., Norman, J., Nordheim, E., 2001. Environmental controls on ground cover species composition and productivity in a boreal black spruce forest. Oecologia 129, 261–270, http://dx.doi.org/10.1007/s004420100719

Black, T.A., den Hartog, G., Neumann, H.H., Blanken, P.D., Yang, P.C., Russell, C., Nesic, Z., Lee, X., Chen, S.G., Staebler, R., 1996. Annual cycles of water vapour and carbon dioxide fluxes in and above a boreal aspen forest. Glob. Change Biol. 2, 219–229.

Blanken, P.D., Black, T.A., Yang, P.C., Neumann, H.H., Nesic, Z., Staebler, R., den Hartog, G., Novak, M.D., Lee, X., 1997. Energy balance and canopy conductance

of a boreal aspen forest: partitioning overstory and understory components. J. Geophys. Res. Atmos. 102, 28915–28927, http://dx.doi.org/10.1029/97JD00193

Burba, G.G., McDermitt, D.K., Grelle, A., Anderson, D.J., Xu, L., 2008. Addressing the influence of instrument surface heat exchange on the measurements of CO_2 flux from open-path gas analyzers. Glob. Change Biol. 14, 1854–1876, http://dx.doi.org/10.1111/j.1365-2486.2008.01606.x

Burba, G., Schmidt, A., Scott, R.L., Nakai, T., Kathilankal, J., Fratini, G., Hanson, C., Law, B., McDermitt, D.K., Eckles, R., Furtaw, M., Velgersdyk, M., 2012. Calculating CO_2 and H_2O eddy covariance fluxes from an enclosed gas analyzer using an instantaneous mixing ratio. Glob. Change Biol. 18, 385–399, http://dx.doi.org/10.1111/j.1365-2486.2011.02536.x

Constantin, J., Grelle, A., Ibrom, A., Morgenstern, K., 1999. Flux partitioning between understorey and overstorey in a boreal spruce/pine forest determined by the eddy covariance method. Agric. For. Meteorol. 98, 629–643.

Detto, M., Montaldo, N., Albertson, J.D., Mancini, M., Katul, G., 2006. Soil moisture and vegetation controls on evapotranspiration in a heterogeneous Mediterranean ecosystem on Sardinia, Italy. Water Resour. Res. 42, W08419, http://dx.doi.org/10.1029/2005WR004693

Euskirchen, E.S., Edgar, C.W., Turetsky, M.R., Waldrop, M.P., Harden, J.W., 2014. Differential response of carbon fluxes to climate in three peatland ecosystems that vary in the presence and stability of permafrost. J. Geophys. Res. Biogeosci. 119, 1576–1595, http://dx.doi.org/10.1002/2014JG002683

Food and Agriculture Organization, 2005. State of the World's Forests 2005. Food and Agriculture Organization of the United Nations, Forest Department, Rome.

Fratini, G., Mauder, M., 2014. Towards a consistent eddy-covariance processing: an intercomparison of EddyPro and TK3. Atmos. Meas. Tech. 7, 2273–2281, http://dx.doi.org/10.5194/amt-7-2273-2014

Fritschen, L.J., Gay, L.W., 1979. Environmental Instrumentation. Springer-Verl., N.Y, 216 pp.

Goulden, M.L., Crill, P.M., 1997. Automated measurements of CO_2 exchange at the moss surface of a black spruce forest. Tree Physiol. 17, 537–542.

Goulden, M.L., Daube, B.C., Fan, S.-M., Sutton, D.J., Bazzaz, A., Munger, J.W., Wofsy, S.C., 1997. Physiological responses of a black spruce forest to weather. J. Geophys. Res. Atmos. 102, 28987–28996, http://dx.doi.org/10.1029/97JD01111

Grant, R.F., Goulden, M.L., Wofsy, S.C., Berry, J.A., 2001. Carbon and energy exchange by a black spruce-moss ecosystem under changing climate: Testing the mathematical model ecosys with data from the BOREAS experiment. J. Geophys. Res. Atmos. 106, 33605–33621, http://dx.doi.org/10.1029/2001JD900064

Hart, S.A., Chen, H.Y.H., 2006. Understory vegetation dynamics of North American boreal forests. Crit. Rev. Plant Sci. 25, 381–397, http://dx.doi.org/10.1080/07352680600819286

Heijmans, M.M.P.D., Arp, W.J., Chapin, F.S., 2004. Carbon dioxide and water vapour exchange from understory species in boreal forest. Agric. For. Meteorol. 123, 135–147, http://dx.doi.org/10.1016/j.agrformet.2003.12.006

Hollinger, D.Y., Kelliher, F.M., Schulze, E.-D., Bauer, G., Arneth, A., Byers, J.N., Hunt, J.E., McSeveny, T.M., Kobak, K.I., Milukova, I., et al., 1998. Forest-atmosphere carbon dioxide exchange in eastern Siberia. Agric. For. Meteorol. 90, 291–306.

Hsieh, C.-I., Katul, G., Chi, T., 2000. An approximate analytical model for footprint estimation of scalar fluxes in thermally stratified atmospheric flows. Adv. Water Resour. 23, 765–772.

Iida, S., Ohta, T., Matsumoto, K., Nakai, T., Kuwada, T., Kononov, A.V., Maximov, T.C., van der Molen, M.K., Dolman, H., Tanaka, H., Yabuki, H., 2009. Evapotranspiration from understory vegetation in an eastern Siberian boreal larch forest. Agric. For. Meteorol. 149, 1129–1139, http://dx.doi.org/10.1016/j.agrformet.2009.02.003

Iwata, H., Ueyama, M., Harazono, Y., Tsuyuzaki, S., Kondo, M., Uchida, M., 2011. Quick recovery of carbon dioxide exchanges in a burned black spruce forest in interior Alaska. SOLA 7, 105–108, http://dx.doi.org/10.2151/sola.2011-027

Iwata, H., Harazono, Y., Ueyama, M., 2012. The role of permafrost in water exchange of a black spruce forest in interior Alaska. Agric. For. Meteorol. 161, 107–115, http://dx.doi.org/10.1016/j.agrformet.2012.03.017

Jarvis, P.G., Massheder, J.M., Hale, S.E., Moncrieff, J.B., Rayment, M., Scott, S.L., 1997. Seasonal variation of carbon dioxide, water vapor, and energy exchanges of a boreal black spruce forest. J. Geophys. Res. Atmos. 102, 28953–28966, http://dx.doi.org/10.1029/97JD01176

Kelliher, F.M., Hollinger, D.Y., Schulze, E.-D., Vygodskaya, N.N., Byers, J.N., Hunt, J.E., McSeveny, T.M., Milukova, I., Sogatchev, A., Varlargin, A., et al., 1997. Evaporation from an eastern Siberian larch forest. Agric. For. Meteorol. 85, 135–147.

Kobayashi, H., Suzuki, R., Nagai, S., Nakai, T., Kim, Y., 2014. Spatial scale and landscape heterogeneity effects on FAPAR in an open-canopy black spruce forest in interior Alaska. IEEE Geosci. Remote Sens. Lett. 11, 564–568, http://dx.doi.org/10.1109/LGRS.2013.2278426

Lloyd, J., Taylor, J.A., 1994. On the temperature dependence of soil respiration. Funct. Ecol. 8, 315–323.

Matthes, J.H., Sturtevant, C., Verfaillie, J., Knox, S., Baldocchi, D., 2014. Parsing the variability in CH_4 flux at a spatially heterogeneous wetland: Integrating multiple eddy covariance towers with high-resolution flux footprint analysis: parsing variability in wetland CH_4 flux. J. Geophys. Res. Biogeosci. 119, http://dx.doi.org/10.1002/2014JG002642

McGuire, A.D., Melillo, J.M., Kicklighter, D.W., Pan, Y., Xiao, X., Helfrich, J., Moore, B., Vorosmarty, C.J., Schloss, A.L., 1997. Equilibrium responses of global net primary production and carbon storage to doubled atmospheric carbon dioxide: sensitivity to changes in vegetation nitrogen concentration. Glob. Biogeochem. Cycles 11, 173–189, http://dx.doi.org/10.1029/97GB00059

Misson, L., Baldocchi, D.D., Black, T.A., Blanken, P.D., Brunet, Y., Curiel Yuste, J., Dorsey, J.R., Falk, M., Granier, A., Irvine, M.R., Jarosz, N., Lamaud, E., Launiainen, S., Law, B.E., Longdoz, B., Loustau, D., McKay, M., Paw, U., Vesala, K.T., Vickers, T., Wilson, D., Goldstein, K.B.A.H., 2007. Partitioning forest carbon fluxes with overstory and understory eddy-covariance measurements: a synthesis based on FLUXNET data. Agric. For. Meteorol. 144, 14–31, http://dx.doi.org/10.1016/j.agrformet.2007.01.006

Moncrieff, J.B., Massheder, J.M., De Bruin, H., Elbers, J., Friborg, T., Heusinkveld, B., Kabat, P., Scott, S., Soegaard, H., Verhoef, A., 1997. A system to measure surface fluxes of momentum, sensible heat, water vapour and carbon dioxide. J. Hydrol. 188, 589–611.

Murray, K.J., Harley, P.C., Beyers, J., Walz, H., Tenhunen, J.D., 1989. Water content effects on photosynthetic response of Sphagnum mosses from the foothills of the Philip Smith Mountains, Alaska. Oecologia 79, 244–250, http://dx.doi.org/10.1007/BF00388484

Nagai, S., Nakai, T., Saitoh, T.M., Busey, R.C., Kobayashi, H., Suzuki, R., Muraoka, H., Kim, Y., 2013. Seasonal changes in camera-based indices from an open canopy black spruce forest in Alaska, and comparison with indices from a closed canopy evergreen coniferous forest in Japan. Polar Sci. 7, 125–135, http://dx.doi.org/10.1016/j.polar.2012.12.001

Naito, A.T., Cairns, D.M., 2011. Patterns and processes of global shrub expansion. Prog. Phys. Geogr. 35, 423–442, http://dx.doi.org/10.1177/0309133311403538

Nakai, T., Shimoyama, K., 2012. Ultrasonic anemometer angle of attack errors under turbulent conditions. Agric. For. Meteorol. 162/163, 14–26, http://dx.doi.org/10.1016/j.agrformet.2012.04.004

Nakai, T., van der Molen, M.K., Gash, J.H.C., Kodama, Y., 2006. Correction of sonic anemometer angle of attack errors. Agric. For. Meteorol. 136, 19–30, http://dx.doi.org/10.1016/j.agrformet.2006.01.006

Nakai, T., Sumida, A., Kodama, Y., Hara, T., Ohta, T., 2010. A comparison between various definitions of forest stand height and aerodynamic canopy height. Agric. For. Meteorol. 150, 1225–1233, http://dx.doi.org/10.1016/j.agrformet.2010.05.005

Nakai, T., Iwata, H., Harazono, Y., 2011. Importance of mixing ratio for a long-term CO_2 flux measurement with a closed-path system. Tellus B 63, 302–308, http://dx.doi.org/10.1111/j.1600-0889.2011.00538.x

Nakai, T., Kim, Y., Busey, R.C., Suzuki, R., Nagai, S., Kobayashi, H., Park, H., Sugiura, K., Ito, A., 2013. Characteristics of evapotranspiration from a permafrost black spruce forest in interior Alaska. Polar Sci. 7, 136–148, http://dx.doi.org/10.1016/j.polar.2013.03.003

Nakai, T., Iwata, H., Harazono, Y., Ueyama, M., 2014. An inter-comparison between Gill and Campbell sonic anemometers. Agric. For. Meteorol. 195/196, 123–131, http://dx.doi.org/10.1016/j.agrformet.2014.05.005

Nilsson, M.-C., Wardle, D.A., 2005. Understory vegetation as a forest ecosystem driver: evidence from the northern Swedish boreal forest. Front. Ecol. Environ. 3, 421–428, http://dx.doi.org/10.1890/1540-9295(2005)003[0421:UVAAFE]2.0.CO;2

Oechel, W.C., Cleve, K.V., 1986. The role of bryophytes in nutrient cycling in the Taiga. In: Cleve III, K.V., Flanagan, F.S.C., Viereck, P.W., Dyrness, L.A.C.T. (Eds.), Forest Ecosystems in the Alaskan Taiga, Ecological Studies. Springer, New York, pp. 121–137.

Ruess, R.W., Hendrick, R.L., Burton, A.J., Pregitzer, K.S., Sveinbjornssön, B., Allen, M.F., Maurer, G.E., 2003. Coupling fine root dynamics with ecosystem carbon cycling in black spruce forests of interior Alaska. Ecol. Monogr. 73, 643–662.

Sampson, D.A., Janssens, I.A., Ceulemans, R., 2006. Under-story contributions to stand level GPP using the process model SECRETS. Agric. For. Meteorol. 139, 94–104, http://dx.doi.org/10.1016/j.agrformet.2006.06.003

Schuur, E.A.G., Trumbore, S.E., 2006. Partitioning sources of soil respiration in boreal black spruce forest using radiocarbon. Glob. Change Biol. 12, 165–176, http://dx.doi.org/10.1111/j.1365-2486.2005.01066.x

Shulski, M., Wendler, G., 2007. The Climate of Alaska. University of Alaska Press.

Sugiura, K., Suzuki, R., Nakai, T., Busey, B., Hinzman, L., Park, H., Kim, Y., Nagai, S., Saito, K., Cherry, J., Ito, A., Ohata, T., Walsh, J., 2011. Supersite as a common platform for multi-observations in Alaska for a collaborative framework between JAMSTEC and IARC. JAMSTEC Rep. Res. Dev. 12, 61–69.

Suzuki, R., Ikawa, H., Kim, Y., Sugiura, K., 2015. Supersite in boreal forest of Alaska established by a Japan and USA Collaboration Study. AsiaFlux Newsl. 38, 14–18.

Tsuyuzaki, S., Kushida, K., Kodama, Y., 2008. Recovery of surface albedo and plant cover after wildfire in a Picea mariana forest in interior Alaska. Clim. Change 93, 517–525, http://dx.doi.org/10.1007/s10584-008-9505-y

Ueyama, M., Harazono, Y., Ohtaki, E., Miyata, A., 2006. Controlling factors on the interannual CO_2 budget at a subarctic black spruce forest in interior Alaska. Tellus B 58, 491–501, http://dx.doi.org/10.1111/j.1600-0889.2006.00205.x

Ueyama, M., Harazono, Y., Kim, Y., Tanaka, N., 2009. Response of the carbon cycle in sub-arctic black spruce forests to climate change: reduction of a carbon sink related to the sensitivity of heterotrophic respiration. Agric. For. Meteorol. 149, 582–602, http://dx.doi.org/10.1016/j.agrformet.2008.10.011

Ueyama, M., Hirata, R., Mano, M., Hamotani, K., Harazono, Y., Hirano, T., Miyata, A., Takagi, K., Takahashi, Y., 2012. Influences of various calculation options on heat, water and carbon fluxes determined by open- and closed-path eddy covariance methods. Tellus B 64B, 19048, http://dx.doi.org/10.3402/tellusb.v64i0.19048

Ueyama, M., Iwata, H., Harazono, Y., 2014. Autumn warming reduces the CO_2 sink of a black spruce forest in interior Alaska based on a nine-year eddy covariance measurement. Glob. Change Biol. 20, 1161–1173, http://dx.doi.org/10.1111/gcb.12434

Ueyama, M., Kudo, S., Iwama, C., Nagano, H., Kobayashi, H., Harazono, Y., Yoshikawa, K., 2015. Does summer warming reduce black spruce productivity in interior Alaska? J. For. Res. 1–8, http://dx.doi.org/10.1007/s10310-014-0448-z

Vickers, D., Mahrt, L., 1997. Quality control and flux sampling problems for tower and aircraft data. J. Atmos. Ocean. Technol. 14, 512–526, http://dx.doi.org/10.1175/1520-0426(1997)014<0512:QCAFSP>2.0.CO;2

Viereck, L.A., Dyrness, C.T., Batten, A.R., Wenzlick, K.J., 1992. The Alaska Vegetation Classification. U.S. Dept. of Agriculture, Forest Service, Pacific Northwest Research Station, Portland, OR, USA, 279 pp.

Vogel, J.G., Valentine, D.W., Ruess, R.W., 2005. Soil and root respiration in mature Alaskan black spruce forests that vary in soil organic matter decomposition rates. Can. J. For. Res. 35, 161–174, http://dx.doi.org/10.1139/x04-159

Xue, B.-L., Kumagai, T., Iida, S., Nakai, T., Matsumoto, K., Komatsu, H., Otsuki, K., Ohta, T., 2011. Influences of canopy structure and physiological traits on flux partitioning between understory and overstory in an eastern Siberian boreal larch forest. Ecol. Model. 222, 1479–1490, http://dx.doi.org/10.1016/j.ecolmodel.2011.01.021.